Vol 16 No 11, November 2007
1009-1963/2007/16(11)/3451-07

Chinese Physics

© 2007 Chin. Phys. Soc.
and IOP Publishing Ltd

Preliminary analysis of impurity transport in HL-2A ohmic discharges*

Chen Wei(陈 伟)†, Cui Zheng-Ying(崔正英), Sun Ping(孙 平),
Huang Yuan(黄 渊), Zhang Peng(张 鹏), Deng Wei(邓 玮), Pan Yu-Dong(潘宇东),
Shi Zhong-Bing(石中兵), Zhou Yan(周 艳), Zheng Yong-Zhen(郑永真), and Yang Qing-Wei(杨青巍)

Southwestern Institute of Physics, Chengdu 610041, *China*

(Received 23 August 2006; revised manuscript received 31 December 2006)

This paper describes the behaviour of impurity transport in HL-2A ohmic discharges. In 2005, small quantities of metallic impurities (Al, Ni and Ti) were successfully injected into HL-2A plasmas by laser blow-off technique, and their progression was followed by the soft x-ray cameras with good spatial and temporal resolutions. The impurity confinement time is estimated from the characteristic decay time of the soft x-ray signal of the injected impurities, and it is about 30–60 ms. The transport coefficients of impurities (including diffusion coefficient and convection velocity) in radial different region have been derived by using a one-dimensional impurity transport code, the results present that diffusion coefficient is much smaller in the central region of plasmas than the outside of it, and it is much larger than that of neoclassical theory predictions; namely, it is anomalous.

Keywords: laser blow-off, impurity transport, soft x-ray emissivity, diffusion coefficient
PACC: 5225F, 5265

1. Introduction

Understanding the impurity behaviour is a critical issue in magnetically confined fusion plasma for well known reasons: impurities in the plasma core enhance radiation losses, and they also affect plasma stability. Especially, with high-Z impurity accumulation, the risk of plasma disruption increases, so that the fusion reactor will be destroyed seriously. Testing the available theoretical predictions still remains one of the main tasks for experimental investigations of impurity transport. The behaviour of impurity is exceedingly complex. How to understand the impurity behaviour in plasmas, so that effective methods of controlling it are able to be obtained, is significant for fusion research and the realization of future reactor. Recently numerical simulation indicates that the transport of impurity is dominated by turbulent processes, as is reported in some papers.[1−8] Experimentally, it is found that the impurity transport is related to temperature gradient, density peaking, magnetic curvature, particle collision and plasma rotation, etc.[2,5,8−11] In some tokamaks, it has been found that the radial transport coefficients of impurities (including diffusion coefficient and convection velocity) strongly increase from the core to the edge. Generally, the coefficient in the core is one order of magnitude smaller than that in the edge. In the core, the transport of impurity is temporally discontinuous when sawtooth oscillations are presented. In the quiet-phase of a sawtooth oscillation the impurity transport is very low. Only during the short crash phase is the transport greatly enhanced.

In the past two decades, many experiments have been performed in different tokamaks (including JET,[11,12] Tore Supra[13−15] and ASDEX-U,[16] etc) by laser blow-off (LBO) technique and gas puffing in order to determine impurity transport coefficients under different q-profile conditions, such as internal transport barrier (ITB), reverse shear and very high (VH) mode, etc. Recently, a comprehensive review on ion transport and confinement was given by the ITER Physics Expert Groups.[17]

In this paper, it is presented that the results of impurity transport studies on HL-2A plasma use LBO technique and impurity transport code in ohmic discharges. The experimental conditions are described in Section 2. The impurity transport simulations are presented in Section 3. The results of experiment and simulation are given in Section 4. The summary and conclusion are contained in Section 5.

*Project supported by the National Natural Science Foundation of China (Grant No 10475022).
†E-mail: chenw@swip.ac.cn

2. Experimental conditions

The HL-2A tokamak (with major radius $R = 1.65\,\mathrm{m}$ and minor radius $a = 0.4\,\mathrm{m}$) is typically operated in the following parameters: plasma current $I_\mathrm{P} = 100 - 400\,\mathrm{kA}$, toroidal field $B_\mathrm{T} = 1 - 2.7\,\mathrm{T}$, discharge duration $t = 1 - 3\,\mathrm{s}$, maximum plateau time $t_\mathrm{au} = 1.5\,\mathrm{s}$, $q_{95} = 3 - 5$, line-average plasma density $< n_\mathrm{e} >= 6\times10^{18} - 6\times10^{19}\,\mathrm{m}^{-3}$, and electron temperature $T_\mathrm{e} = 600 - 1200\,\mathrm{eV}$. It can be performed in divertor and limiter configurations with similar plasma parameters.

Small quantities of metallic impurities (Al, Ni and Ti) are injected by a LBO system on HL-2A.[18] The laser source is provided by a Nd-glass laser (wave length 1053 nm). The pulse is about 8–30 ns and single pulse power is selected from 3 to 5 J. The target has a 2 μm coating of impurities on a glass slide, of which a region with diameter of 3–6 mm was ablated. The number of atoms ablated each time is about 10^{16}–10^{18}. The criterion for impurity injection is that the change in the main plasma parameters due to injection is very small and non-perturbing. Experimentally, the injected impurity density is found to be of the order of $10^{16}\,\mathrm{m}^{-3}$, and its influence on the plasma current and electron density can be neglected.

The evolution of impurity ions in the main plasmas is followed by a 100 channel soft x-ray multicamera system (5 arrays, 20 channels for each array)[19] of which the energy range of its detector is 1–10 keV. The spatial and temporal resolution of the system is 2.5 cm and 10 μs respectively. Time dependent emission profiles of impurity ions are derived from the local soft x-ray emissions reconstructed by a tomographic technique. Meanwhile, the evolution of total radiation losses is measured with multichord bolometric arrays (3 arrays, 16 channels for each array). The detector is Absolute Extreme Ultra Violet (AXUV) silicon photodiodes of which the energy range is from 1 eV to 10 keV. The spatial and temporal resolutions of the system are 2.5 cm and 50 μs respectively. In addition, the evolution of impurity line radiation is observed by a monochromator in the VUV spectral range.[20]

Aluminium is injected during quasi-steady state discharge phase, as it appears clearly for a typical shot at $t = 800\,\mathrm{ms}$ in Fig.1 (shot 4018), where the current I_p, loop-voltage V_loop, the central electron density $< n_\mathrm{e} >$ (ρ is normalized radius), the brightness of soft x-ray signal E_sx (normalized), total radiation losses E_BOL (normalized, from Bolometer), the line brightness of Al XI (wave length $\lambda = 55.0\,\mathrm{nm}$) E_L (normalized, from VUV) and the temperature T_e (from ECE) are presented.

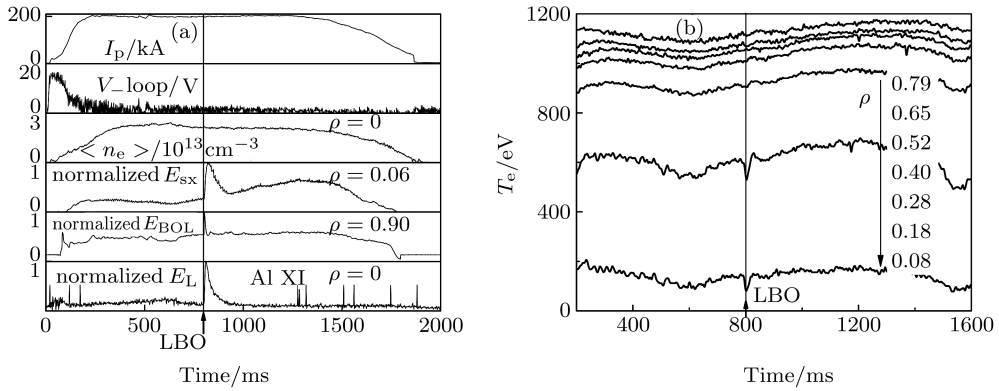


Fig.1. Time evolutions of plasma current I_p, loop-voltage $V_$loop, central electron density $< n_\mathrm{e} >$, brightness of soft x-ray signal E_sx (normalized), total radiation losses E_BOL (normalized), line brightness of Al XI E_L (normalized) and temperature T_e, for HL-2A shot 4018.

3. Impurity transport simulation

The impurity transport code (STRAHL) was introduced around 1986 from Europe, which was supported by International Atomic Energy Agency (IAEA) projects, and it was successfully used on HL-1M tokamak.[21,22] Over the years, the code has gone through several modifications including transplanting from DOS to Window operation system and supplementing simulations of soft x-ray and total radiation losses.

The radial particle flux through a magnetic flux surface is governed by the continuity equation. The

impurity particle flux density Γ_z is given by the formula:[23]

$$\frac{\partial N_z}{\partial t} + \nabla \cdot \Gamma_z = Q_{zt}. \quad (1)$$

Where N_z is the particle density of impurity in ion stage Z, and Q_{zt} is the sum of all particle sources and sinks.

The impurity flux density Γ_z is expressed as the sum of both diffusive and convective terms:

$$\Gamma_z = -D_z \frac{\mathrm{d}N_z}{\mathrm{d}r} + V_z N_z. \quad (2)$$

Where D and V are radial diffusion coefficients and convection velocities respectively. D and V include a neoclassical part and an anomalous part. The neoclassical part of V is the so-called Ware pinch velocity[24] $V_{\mathrm{ware}} = -c\dfrac{E_\psi}{B_\theta}$ (where c is constant, E_ψ is the toroidal electric field and B_θ is the poloidal magnetic field), and its direction is inward. The anomalous part of D and V is related to temperature gradient, density peaking, magnetic curvature, particle collision and plasma rotation, etc. It has not consistent conclusion that they contribute to the anomalous part. In the analysis, the coefficients D and V are assumed to be independent of ion stage and do not vary with time, and $V = 2S\dfrac{D\ r}{a^2}$ (where a is the mesh last radius, a few centimetres out the last closed flux surface, constant S is about 0.5–2). The source and sink term Q_{zt} couples the transport equation is made up of the ionization I_z, recombination R_z, charge exchange C_z, parallel loss L_z and outer source/sink Q_z. They can be respectively written as

$$I_z = N_{\mathrm{e}}(N_{z-1}S_{z-1} - N_z S_z), \quad (3)$$

$$R_z = N_{\mathrm{e}}(N_{z+1}\alpha_z - N_z\alpha_{z-1}), \quad (4)$$

$$C_z = N_{\mathrm{H}}(N_{z+1}\alpha_{z+1}^{cx} - N_z\alpha_z^{cx}), \quad (5)$$

$$L_z = -\frac{N_z}{\tau_\parallel}. \quad (6)$$

Where N_{e} and N_{H} are electron density and hydrogen density, S_z, α_z, α_z^{cx} and $\tau_\parallel$ are ionization coefficient, recombination coefficient, charge exchange coefficient and parallel loss time respectively.

Assumed an invariable source (S_0) of impurity locating at the edge of plasma, the density (N_0) of neutral impurity atoms due to ionization entering plasma decays as follows:

$$N_0(r) = N_0(R)\frac{R}{r}\exp\left(-\int_r^R N_{\mathrm{e}}S_0\mathrm{d}r/v_0\right), \quad (7)$$

where v_0 is initial velocity of impurity, R is distance of impurity source to plasma centre. Therefore, the number (Q_0) of ions produced per unit time per unit length is:

$$Q_0 = 2\pi\int_0^R N_0(r)N_{\mathrm{e}}S_0 r\mathrm{d}r. \quad (8)$$

For the calculations of ionization, recombination and charge exchange rate coefficients, the radial profiles of electron density and electron temperature have to be specified, while the relevant rate coefficients are taken from the atomic database. The hydrogen density is calculated from the impurity densities and the given electron density using condition of quasi-neutrality.

In scrape-off layer (SOL), electron temperature $T_{\mathrm{ea}}(r)$ and electron density $N_{\mathrm{ea}}(r)$ decay as follows:

$$T_{\mathrm{ea}}(r) = T_{\mathrm{e}}(a)\exp[(a-r)/\lambda_{\mathrm{T}}], \quad (9)$$

$$N_{\mathrm{ea}}(r) = N_{\mathrm{e}}(a)\exp[(a-r)/\lambda_{\mathrm{n}}], \quad (10)$$

where λ_{T} and λ_{n} are the decay lengths of temperature and density respectively.

The neoclassical transport coefficients[25] are the sum of a classical (CL), a Pfirsch–Schluter (PS) and a banana plateau (BP) terms. The three contributions are calculated with the relevant formula.[26] The anomalous diffusion coefficient is assumed to have the form as follows:

$$D(r) = D(a)\left[1 + \alpha\left(\frac{r}{a}\right)^\beta\right]/(1+\alpha). \quad (11)$$

The energy losses due to impurities consist of ionization, line radiation, recombination and Bremsstrahlung for tokamak plasma. The corresponding power densities of these four kinds of emission are listed below (all in unit of $\mathrm{W{\cdot}m^{-3}}$).[27]

$$\begin{aligned} p_{\mathrm{i}} &= c_1\sum_{z=1}^{M-1} N_{\mathrm{e}}N_z S_z\left(\chi_z + \frac{3}{2}T_{\mathrm{e}}\right) + p_{\mathrm{r}}, \\ p_{\mathrm{r}} &= c_2\sum_{z=1}^{M-1} N_{\mathrm{e}}N_{z+1}\alpha_z T_{\mathrm{e}}, \\ p_{\mathrm{br}} &= c_3 z_{\mathrm{eff}} N_{\mathrm{e}}^2 T_{\mathrm{e}}^{1/2}, \\ p_{\mathrm{l}} &= c_4 N_{\mathrm{e}}T_{\mathrm{e}}^{1/2}\sum_{z=2}^{M-1} N_z\sum_{l=1}^{L} C_{zl}\exp\left(-\frac{\chi_{\mathrm{ex}}}{T_{\mathrm{e}}}\right), \end{aligned} \quad (12)$$

where M is the atomic number, χ_z is the ionization energy, z_{eff} is the effective ionic charge, χ_{ex} is the excitation energy, $c_1 - c_4$ are constants and C_{kl} are coefficients in the Ref.[27].

The plasma parameters (e.g. electron temperature T_e and electron density N_e) are measured accurately, and the transport coefficients are given by the formula (11). Then, the data points are read into the simulation code. By finely adjusting their profiles until a good agreement is achieved between the experimental and the simulation data, a successful model for impurity transport is produced. In this way, the transport coefficients of impurities in radial different region have been derived, and the results are considered to determine in the experiment.

4. Experimental results

Aluminium is successfully injected into plasmas at 800 ms by LBO technique for HL-2A shot 4057. After Al has been injected, the soft x-ray signals at $\rho = 0.06$ and $\rho = 0.38$ are shown in Fig.2. Only the contribution from injected impurity (Al) is taken into account and the background level of plasma before LBO has been subtracted. This can be done because the background radiation is nearly constant, apart from the sawtooth activity that represents only a minor perturbation in comparison with the extra radiation due to the injected impurities.

From Fig.2, it is found that the first inward and then outward movements of the injected impurities and the process of impurity accumulation can be observed between two dot lines. During the rising phase of the soft x-ray signal, the impurities enter regions of higher electron density and higher electron temperature, and the sawteeth are inverted at 805.6 and 813.2 ms, which suggests that the flow of impurities is inward from the edge to the central region of plasmas at the time of the sawtooth crash. Similarly, during the decreasing phase of the soft x-ray signal, the impurities continuously diffuse out, and the sawteeth are inverted at 821.2 and 829.4 ms, this implies that the flow of impurities is outward from the central region to the edge at the time of the sawtooth crash.

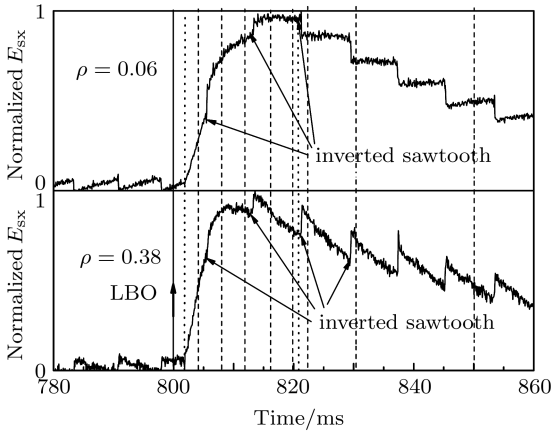


Fig.2. Time evolutions of the local soft x-ray signal E_{sx} (normalized) at normalized radius 0.06 and 0.38, for HL-2A shot 4057. The background radiation before LBO has been subtracted. The vertical dash lines express the times for the tomographic reconstructions shown in Fig.3. The vertical dot lines from left to right indicate the process of impurity accumulation.

Figure 3 shows the tomographic reconstructions of the soft x-ray emissivity distributions for the times indicated by the vertical dash lines in Fig.2, and corresponding to 804, 808, 812 and 816 ms during the rising phase of the soft x-ray signal, and to 820, 822, 830 and 850 ms during the decreasing phase of the soft x-ray signal. Figure 4 shows the soft x-ray emissivity distributions along a horizonal central chord.

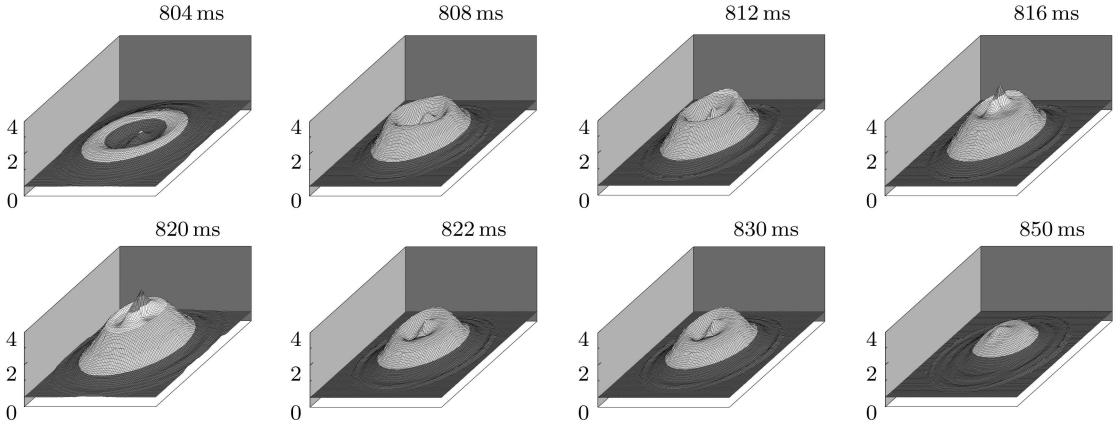


Fig.3. Time evolutions of the local soft x-ray emissivity distribution following impurity injection as reconstructed from the line integrated measurements for the times indicated and corresponding to the vertical dash lines in Fig.2. The background radiation before LBO has been subtracted.

From Figs.3 and 4, in the early time of injected impurities, the impurities propagate inwards, and the soft x-ray emissivity distribution is hollow, and has an asymmetric profile. This indicates that impurity transport is poloidally asymmetric, and the impurity radiation at lower field side is stronger. By the formula $x_h(t) = \sum_i x_i(h)\exp(-t/\tau_i)$ (where $x_h(t)$ represents the soft x-ray signal at the coordinate (h) identifying the line of sight, $x_i(h)$ is spatial component, and τ_i is relaxation time. τ_1 is identified as the impurity confinement time $\tau_{\rm p}$, whereas τ_2 is connected with the initial ingress phase of the injected impurity, see the Refs.[13, 28]), the impurity confinement time $\tau_{\rm p}$ is determined about 30 ms for shot 4057. The similar results can be obtained by the analysis of the experimental data.

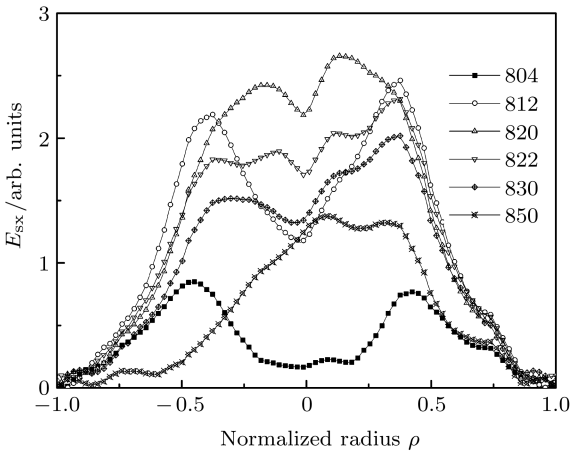


Fig.4. Time evolutions of the local soft x-ray emissivity distribution along a horizontal central chord for different times. The background radiation before LBO has been subtracted.

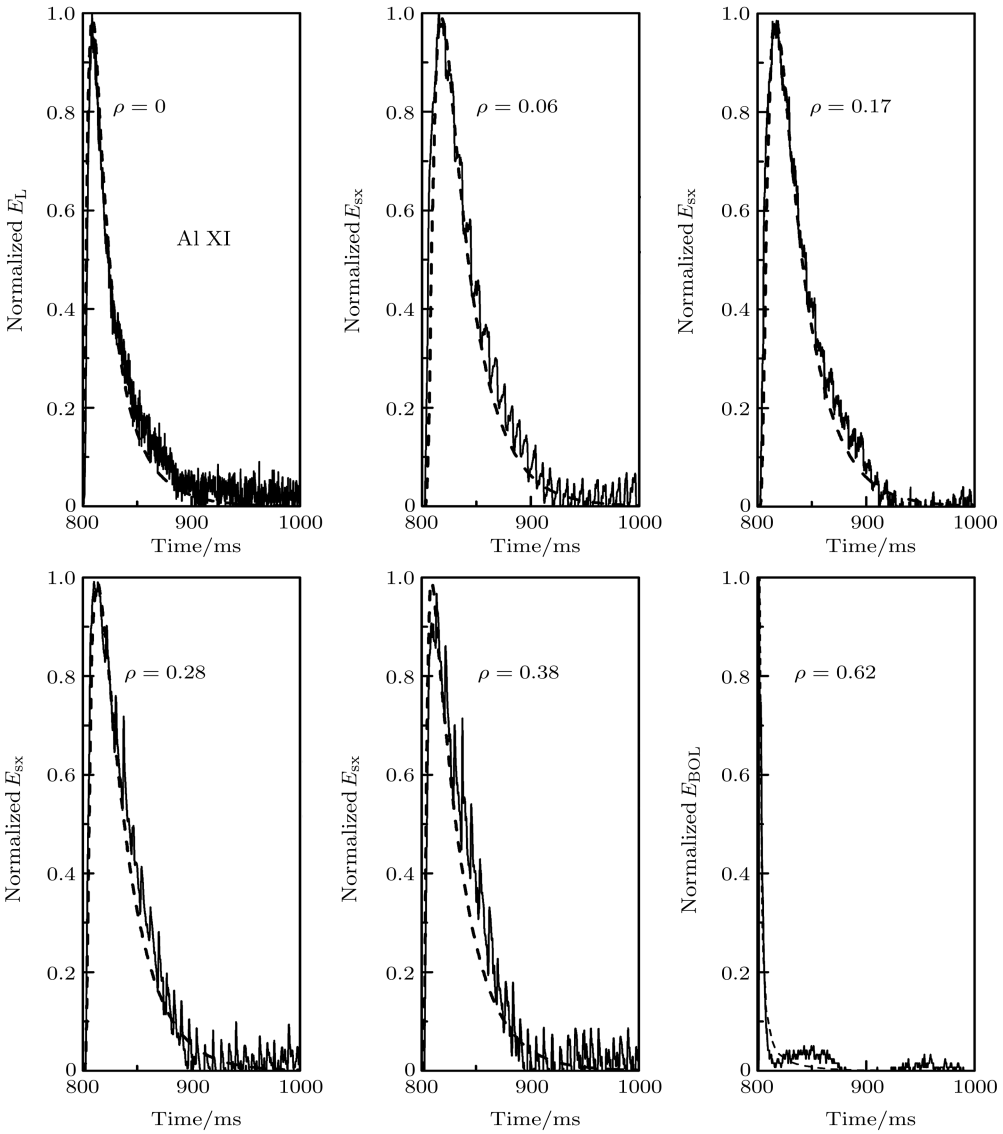


Fig.5. Time evolutions of the soft x-ray brightness, total radiation losses, and line brightness of Al XI for HL-2A shot 4057. The background radiation before LBO has been subtracted. The simulated curves are also shown.

The transport coefficients of impurities (including diffusion coefficient D and convection velocity v) in radial different regions have been derived by using impurity transport code. The brightness of soft x-ray signal $E_{\rm sx}$ (normalized), total radiation losses $E_{\rm BOL}$ (normalized), and line brightness of Al XI $E_{\rm L}$ (normalized) are shown in Fig.5. The solid line and dash line are experimental and simulative result respectively.

Figure 6 shows the transport coefficients of impurities in radial different region. The values of D are 0.82, 0.90 and 2.15 $\rm m^2/s$ at $\rho = 0, 0.5, 0.8$ in the discharge. They are much larger than those of the neoclassical predictions (by using the neoclassical transport formula estimation, the neoclassical maximum of D in the central region of plasma is less than 0.05, and about $0.1\rm m^2/s$ in the edge). This indicates that the transport of impurity is anomalous. At present, the transport parameters beyond $\rho = 0.8$ are inaccurate, because the complex processes in SOL are not considered in detail in the code.

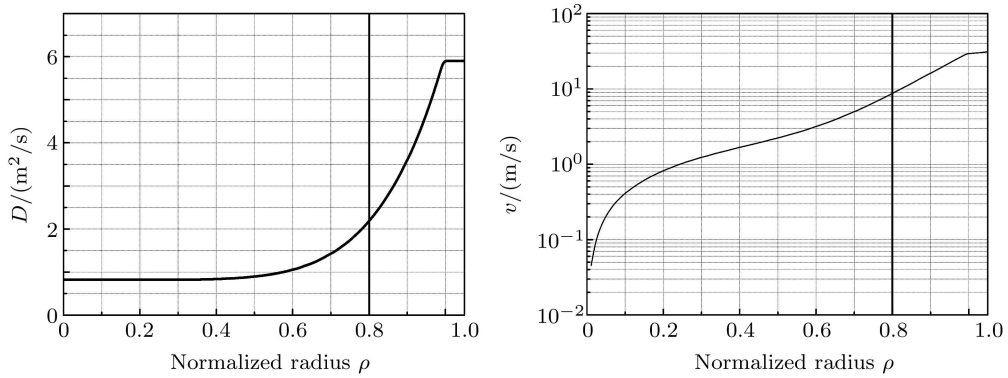


Fig.6. The profiles of the diffusion coefficient D and convection velocity v for HL-2A shot 4057.

5. Summary and conclusion

The behaviour of impurity transport is illuminated by using the LBO technique and impurity transport code in HL-2A ohmic discharges. The experimental results clearly show that the design parameters of laser target and films are quite reasonable. After impurities have been injected, it is found experimentally that the movements of the injected impurities are first inward and then outward by using the soft x-ray cameras. During the rising phase of the soft x-ray signal, the flow of impurities is inward from the edge to the central region of plasmas at the time of the sawtooth crash. Similarly, during the decreasing phase of the soft x-ray signal, the flow of impurities is outward from the central region to the edge at the time of the sawtooth crash. In the early time of injected impurities, the soft x-ray emissivity distribution is hollow, and has an asymmetric profile. It indicates that impurity transport is poloidally asymmetric. Transport of impurity is enhanced greatly during sawtooth crashes. Impurity confinement time is about 30–60 ms on HL-2A. By impurity transport code, diffusion coefficient D and convection velocity v have been determined on HL-2A ohmic discharges. In the central region of plasma ($0 \le \rho < 0.5$), the typical values of D and v are $0.5 - 1.0\rm m^2/s$ and $0.0 - 3.0\rm m/s$ respectively. However, in the range of $0.5 \le \rho < 0.8$, the values are $1.0 - 2.5\rm m^2/s$ and $3.0 - 10.0\rm m/s$. They are much larger than those of the neoclassical theory predictions, and impurity transport is anomalous. The anomalous behaviour of impurity transport will be deeply researched by using theory and experiment.

The author is grateful to Professor Yan Long-Wen for useful suggestions, and would like to thank the assistance of the HL-2A group.

References

[1] Naulin V, Nycander J and Rasmussen J J 1998 *Phys. Rev. Lett.* **81** 4148

[2] Stroth U, Geist T, Koponen J P T, Hartfuß H J, Zeiler P, the ECRH and W7-AS team 1999 *Phys. Rev. Lett.* **82** 928

[3] Hoang G T, Bourdelle C, Pegourie B, Schunke B, Artaud J F, Bucalossi J, Clairet F, Fenzi-Bonizec C, Garbet X,

Gil C, Guirlet R, Imbeaux F, Lasalle J, Loarer T, Lowry C, Travere J M, Tsitrone E and Tore Supra Team 2003 *Phys. Rev. Lett.* **90** 155002

[4] Garbet X, Garzotti L, Mantica P, Nordman H, Valovic M, Weisen H and Angioni C 2003 *Phys. Rev. Lett.* **91** 035001

[5] Hoang G T, Bourdelle C, Garbet X, Artaud J F, Basiuk V, Bucalossi J, Clairet F, Fenzi-Bonizec C, Gil C, Segui J L, Travere J M,Tsitrone E and Vermare L 2004 *Phys. Rev. Lett.* **93** 135003

[6] Bourdelle C 2005 *Plasma Phys. Control. Fusion* **47** A317-A326

[7] Hoang G T, Bourdelle C, Garbet X, Pegourie B, Artaud J F, Basiuk V, Bucalossi J, Fenzi-Bonizec C, Clairet F, Eriksson L G, Gil C, Guirlet R, Imbeaux F, Lasalle J, Lowry C, Schunke B, Segui J L, Travere J M and Vermare L 2006 *Nucl. Fusion* **46** 306

[8] Garbet X, Mantica P, Angioni C, Asp E, Baranov Y, Bourdelle C, Budny R, Crisanti F, Cordey G, Garzotti L, Kirneva N, Hogeweij D, Hoang T, Imbeaux F, Joffrin E, Litaudon X, Manini A, Mcdonald D C, Nordman H, Parail V, Peeters A, Ryter F, Sozzi C, Valovic M, Tala T, Thyagaraja A, Voitsekhovitch I, Weiland J, Weisen H, Zabolotsky A and the JET EFDA Contributors 2004 *Plasma Phys. Control. Fusion* **46** B557

[9] Angioni C, Peeters A G, Pereverzev G V, Ryter F, Tardini G and ASDEX-U Team 2003 *Phys. Rev. Lett.* **90** 205003

[10] Tanaka K, Michael C, Sanin A L, Vyacheslavov L N, Kawahata K, Murakami S, Wakasa A, Okajima S, Yamada H, Shoji M, Miyazawa J, Morita S, Tokuzawa T, Akiyama T, Goto M, Ida K, Yoshinuma M, Yamada I, Yokoyama M, Masuzaki S, Morisaki T, Sakamoto R, Funaba H, Inagaki S, Kobayashi M, Komori A and LHD experimental group 2006 *Nucl. Fusion* **46** 110

[11] Chen H, Hawkes N C, Ingesson L C, Peacock N J and Haines M G 2001 *Nucl. Fusion* **41** 31

[12] Pasini D, Giannella R, Taroni L L, Mattioli M, Denne-Hinnov B, Hawkes N, Magyar G and Weisen H 1992 *Plasma Phys. Control. Fusion* **34** 677

[13] Mattioli M, Giannella R, Myrnas R, Demichelis C, Denne-Hinnov B, Dubok De Wit T and Magyar G 1995 *Nucl. Fusion* **35** 1115

[14] Mattioli M, De-Michelis C and Monier-Garbet P 1995 *Nucl. Fusion* **35** 807

[15] Mattioli M, De-Michelis C and Pecquet A L 1998 *Nucl. Fusion* **38** 1629

[16] Dux R and Peeters A G 1999 *Nucl. Fusion* **39** 1509

[17] ITER Physics Basis 1999 *Nucl. Fusion* **39** 2175

[18] Cui Z Y, Huang Y, Sun P, Zheng Y Z, Shi P L, Lu J, Fu B Z, Zhang P, Pan Y D, Dong Y B, Deng W, Yang Q W and Ding X T 2006 *Chin. Phys. Lett.* **23** 2143

[19] Liu Y, Peterson B J, Dong Y B, Pan Y D and Deng W 2006 *Plasma Science & Technology* **8** 41

[20] Cui Z Y, Sun P, Pan Y D, Li W, Wang Q M and Duan X R 2006 *Plasma Science & Technology* **8** 61

[21] Feng X Y, Wang Z H, Wang E Y, Chen J, Luo J L, Yu Z R, Zhong Y Z, Dong J F, Li K H, Guo G C, Deng Z C, Shi M L, Yan J C, Zhen Y J and Burhenn R In: 1997 Schittenhelm M, eds. *ECA. 24th European Physical Society Conference on Controlled Fusion and Plasma Physics,* Kongresshaus Berchtegaden, Germany (Geneva: European Physical Society) Vol.21A p657

[22] Chen J, Feng X Y, Wang Z H, Burhenn R, Wang E Y, Luo J L, Dong J F, Zhong Y Z, Qian S J and Yan J C In: 1997 Schittenhelm M, eds. *ECA.24th European Physical Society Conference on Controlled Fusion and Plasma Physics,* Kongresshaus Berchtegaden, Germany (Geneva: European Physical Society) Vol.21A p649

[23] Koponen J P T, Geist T, Stroth U, Fiedler S, Hartfuss H J, Heinrich O, Walter H, ECH Group and W7-AS Team 2000 *Nucl. Fusion* **40** 365

[24] Ware A A 1970 *Phys. Rev. Lett.* **25** 916

[25] Hirshman S P and Sigmar D J 1981 *Nucl. Fusion* **21** 1079

[26] Dux R, Peeters A G, Gude A, Kallenbach A, Neu R and ASDEX-U Team 1999 *Nucl. Fusion* **39** 1509

[27] Tazima T, Nakamura Y and Inoue K 1977 *Nucl. Fusion* **17** 419

[28] Leung W K, Rowan W L, Wiley J C, Bravenec R V, Gentle K W, Hodge W L, Patterson D M, Phillips P E, Price T R and Richards B 1986 *Plasma Phys. Control. Fusion* **28** 1753